CIRRUS CLOUDS AND ICE SUPERSATURATED REGIONS IN A GLOBAL CLIMATE MODEL

Ulrike Lohmann[1*], Peter Spichtinger[1], Stephanie Heidt[1], Thomas Peter[1] and Herman Smit[2]

[1] ETH Zurich, Institute for Atmospheric and Climate Science, Switzerland
[2] Forschungszentrum Jülich, Jülich, Germany

1 ABSTRACT

At temperatures below 238 K cirrus clouds can form by homogeneous and heterogeneous ice nucleation mechanisms. A parameterization for homogeneous freezing that includes the effects of aerosol size (Kärcher and Lohmann, 2002) was implemented in the ECHAM5 global climate model (Lohmann et al., 2007). We assume that the soluble/mixed Aitken, accumulation and coarse mode aerosols are available for homogeneous freezing. For the heterogeneous freezing simulations, we consider the immersed dust particles to act as ice nuclei initiating freezing at 130% relative humidity with respect to ice. When changing the mass accommodation coefficient of water vapor on ice crystals from 0.5 in the standard ECHAM5 simulation to 0.005 as suggested by previous laboratory experiments, the number of ice crystals increases by one order of magnitude caused by the delayed relaxation of supersaturation. As the ice water path changes only by 20% in the global annual mean, the ice crystals are much smaller so that the shortwave and longwave cloud forcing at the top-of-the atmosphere change by 12 and 16 W m^{-2}, respectively. The impact of heterogeneous freezing instead of homogeneous freezing is much weaker with changes in the global annual shortwave and longwave cloud forcing of 0.6 and 1.1 W m^{-2}, respectively.

*ulrike.lohmann@env.ethz.ch

2 INTRODUCTION

Cirrus clouds can form by homogeneous and heterogeneous ice nucleation mechanisms at temperatures below 238 K. They cover on average 30% of the Earth surface and thus are important modulators of the radiation budget. Thin cirrus are semi-transparent in the solar radiation spectrum, allowing the majority of the solar radiation to be transmitted to the surface. Because of their cold temperatures, they emit the absorbed infrared radiation at much colder temperatures than the Earth's surface and thus cause a warming of the Earth-atmosphere system (Chen et al., 2000). Only for thick cirrus, the reflected shortwave and emitted longwave radiation are comparable in magnitude.

While homogeneous freezing of supercooled aqueous phase aerosol particles is rather well understood, understanding of heterogeneous ice nucleation is still in its infancy. A change in the number of ice crystals in cirrus clouds could exert a cloud albedo effect in the same way that the cloud albedo effect acts for water clouds. It refers to the change in the radiative forcing at the top-of-the-atmosphere caused by an enhancement in cloud albedo from anthropogenic aerosols that lead to more and smaller cloud droplets for a given cloud water content. In addition, a change in the cloud ice water content could exert a radiative effect in the infrared. The magnitude of these effects in the global mean has not yet been fully established, but the development of physically based parametrization schemes of cirrus formation for use in global models led to significant progress in understanding underlying mechanisms of aerosol-induced cloud modifications (Kärcher and Lohmann, 2002; Liu and Penner, 2005; Kärcher et al., 2006; Liu et al., 2007).

A global climate model study concluded that a cloud albedo effect based solely on ubiquitous homogeneous freezing is small globally (Lohmann and Kärcher, 2002). This is expected to also hold in the presence of heterogeneous IN that cause cloud droplets to freeze at relative humidities over ice close to homogeneous values (above 130-140%) (Kärcher and Lohmann, 2003). Efficient heterogeneous IN, however, would be expected to lower the relative humidity over ice, so that the climate effect may be larger (Liu and Penner, 2005). In situ measurements reveal that organic-containing aerosols are less abundant than sulphate aerosols in ice cloud particles, suggesting that organics do not freeze preferentially (Cziczo et al., 2004). A model study explains this finding by the disparate water uptake of organic aerosols, and suggests that organics are unlikely to significantly modify cirrus formation unless they are present in very high concentrations (compared with sulphate-rich particles) at low temperatures (Kärcher and Koop, 2005). Recent high-altitude aircraft measurements indicated the presence of rather large, thin hexagonal plate ice crystals near the tropical tropopause in very low concentrations that are suggested to result from ice nucleation on effective heterogeneous nuclei at low ice supersaturations (Jensen et al., 2008).

Besides nucleation effects, ice growth impedances were recently found to lead potentially to high supersaturations within cirrus clouds (Peter et al., 2006). The role of physicochemical processes affecting the accommodation coefficient of water vapour on ice and of water vapour on aerosols is presently unclear. These effects could be related to unknown intrinsic properties of the ice substance at the extreme temperatures at high tropical cirrus levels, or due to natural or anthropogenic species on the ice surface (Wood et al., 2001). Magee et al. (2006) suggested that assuming accommodation coefficients between 0.0045 and 0.0075 was necessary to match laboratory data of ice crystal growth at temperatures between -40 and -60°C and variable supersaturations.

The properties and global distributions of ice supersaturated regions (ISSRs) were discovered during the last years, e.g., Spichtinger et al. (2003); Gettelman et al. (2006). ISSRs are potential formation regions of cirrus and persistent contrails. They are rather ubiquitous (Spichtinger et al., 2003) in the upper tropical troposphere, with frequencies of occurrence even exceeding 50% of the time at 150 hPa. Immler et al. (2008) evaluated lidar data over Northern Germany and concluded that 50% of the air at 11-12 km was supersaturated with respect to ice.

In this paper, we discuss the impact of heterogeneous freezing versus homogeneous freezing and of variations in the deposition coefficient on cirrus cloud properties and ice supersaturation.

3 MODEL DESCRIPTION

We use the ECHAM5 general circulation model (GCM) (Roeckner et al., 2003) to estimate the importance of aerosol effects on convective clouds. The version of ECHAM5 used in this study includes the double-moment aerosol scheme ECHAM5-HAM that predicts the aerosol mixing state in addition to the aerosol mass and number concentrations (Stier et al., 2005). The size-distribution is represented by a superposition of log-normal modes including the major global aerosol compounds sulfate, black carbon, organic carbon, sea salt and mineral dust.

The stratiform cloud scheme consists of prognostic equations for the water phases (vapor, liquid, solid), bulk cloud microphysics (Lohmann and Roeckner, 1996), and an empirical cloud cover scheme (Sundqvist et al., 1989). The microphysics scheme includes phase changes between the water components and precipitation processes (autoconversion, accretion, aggregation). Moreover, evaporation of rain and melting of snow are considered, as well as sedimentation of cloud ice. It also includes prognostic equations of the number concentrations of cloud droplets and ice crystals in stratiform and convective clouds and has been coupled to the aerosol scheme ECHAM5-HAM (Lohmann, 2008). In the standard simulation that assumes cirrus cloud formation solely by homogeneous freezing, ECHAM5-hom (Table 1) an accommodation coefficient α for depositional growth of water vapor onto ice crystals of 0.5 is employed (Kärcher and Lohmann, 2002).

The version of the model used here includes a few changes. Ice crystals are now regarded as plates as this is a more realistic shape for ice crystals in clouds within the mixed-phase regime between 0 and -35° C than assuming spherical crystals (Pruppacher and Klett, 1997). This affects the depositional growth equation where the capacitance C now becomes $C = 2r/\pi$ instead of $C = r$, where r is the equivalent crystal radius:

$$Q_{dep} = \left(\frac{\partial q_i}{\partial t}\right)_{dep} = 4\pi C\alpha A_T f_{Re}(S_i - 1)N_i \quad (1)$$

Here q_i is the ice water mixing ratio, f_{Re} is the ventilation factor as a function of the Reynolds number, S_i is the saturation ratio over ice at the beginning of the time step, N_i is the ice crystal number concentration, and A_T is defined as:

$$A_T = \left(\rho\left[\frac{L_s}{k_a T}\left\{\frac{L_s}{R_v\,T} - 1\right\} + \frac{R_v T}{D_v e_{si}}\right]\right)^{-1},$$

Here T is the temperature, L_s is the latent heat of sublimation, k_a is the thermal conductivity of air, R_v is the gas constant of water vapor, D_v is the diffusivity of water vapor in air, and e_{si} is the saturation vapor pressure over a plane ice surface.

Assuming ice crystals to be plates also changes the calculation of the ice crystal effective radius r_i, which is now given as described in Pruppacher and Klett (1997) for a plate of type P1a (in μm):

$$r_i = 0.5 \cdot 10^4 \left(\frac{IWC}{0.0376 N_i}\right)^{0.302} \quad (2)$$

where N_i is the ice crystal number concentration in m^{-3} and IWC is the ice water content in g m^{-3}.

The fall velocity of ice crystals has been changed to one appropriate for monodisperse crystals, that vary their shapes with increasing size following Spichtinger and Gierens (2008). Assuming monodisperse crystals is consistent with the other formulations for microphysical processes in the model and allows us to use the same fall velocity for number and mass.

Also, the critical thickness necessary for the onset of convective precipitation p_c has been changed. While it was set to 150 hPa over oceans and 300 hPa over land in the simulations described in Lohmann (2008), here we use an observed relationship between the depth above cloud base at which precipitation is initiated, p_c in Pa, as a function of the cloud droplet number concentration N_l in cm^{-3} based on data obtained in the Amazon (Freud et al., 2008) and Freud, pers. comm. 2007:

$$p_c = (293 + 2.73 N_l) g\rho \quad (3)$$

where g is the acceleration due to gravity and ρ is the air density.

3.1 Set-up of the simulations

The ECHAM5 simulations have been carried out in T42 horizontal resolution (2.8125° × 2.8125°) and 19 vertical levels with the model top at 10 hPa and a timestep of 30 minutes. All simulations used climatological sea surface temperature (SST) and sea-ice extent. They were simulated for 5 years after an initial spin-up of 3 months using aerosol emissions for the year 2000.

The reference simulation ECHAM5-hom is conducted such that the global annual mean radiation budget is balanced to within 1 W m^{-2} at the top-of-the-atmosphere (TOA) and that the values of the shortwave and longwave cloud

Tab. 1: Sensitivity Simulations

Simulation	Description
ECHAM5-hom	Simulation with ECHAM5-HAM coupled to the double-moment cloud microphysics scheme for stratiform and convective clouds (Lohmann, 2008) assuming that all cirrus cloud form by homogeneous freezing
ECHAM5-het	As ECHAM5-hom, but assuming that all immersed dust particles are available as immersion freezing nuclei initiating freezing at 130% relative humidity with respect to ice
ECHAM5-alpha	As ECHAM5-hom, but decreasing the accommodation coefficient from 0.5 to 0.005

forcings are within the uncertainty of the radiative flux measurements of $\pm$ 5 W m^{-2} as reported by Kiehl and Trenberth (1997). This required changing the critical radius above which aerosols could possible act as CCN from 35 nm to 30 nm for stratiform clouds and from 25 nm to 20 nm for convective clouds.

In the sensitivity experiment ECHAM5-het (Table 1), homogeneous freezing of potentially all supercooled soluble/mixed aerosol particles was replaced by heterogeneous immersion freezing following Kärcher and Lohmann (2003). As there is currently no consensus on the freezing ability of black carbon, e.g. (Möhler et al., 2005; Dymarska et al., 2006), we limit the number of heterogeneous ice nuclei to the number of immersion mode dust particles as described by Hoose et al. (2008). In simulation ECHAM5-alpha, the accommodation coefficient of water vapor on ice crystals has been decreased from 0.5 in simulations ECHAM5-hom and ECHAM5-het to 0.005 as suggested by laboratory experiment (Magee et al., 2006).

4 MODEL EVALUATION

Validation of the coupled aerosol-cloud microphysics scheme in stratiform clouds is described in Lohmann et al. (2007). Here we focus on the validation of ice supersaturated regions (ISSR) and cirrus clouds.

An overview of the global-mean cloud properties is given in Table 2. The most striking difference between ECHAM5-alpha and ECHAM5-hom is the tenfold increase in the number concentration in ice crystals in ECHAM5-alpha. This results from the slower depositional growth that cannot deplete the supersaturation effectively. In fact, the water vapor has increased by 2.7 kg m^{-2} in the global mean. As a result of the slower depletion of supersaturation, more ice crystals are nucleated. These ice crystals do not grow as large thus slowing down the precipitation formation rate and increasing the amount of cloud ice that remains within the atmosphere (cf. Table 2). This reduces the global mean precipitation by 0.39 mm/d in ECHAM5-alpha as compared to ECHAM5-hom. The more numerous and smaller ice crystal scatter more radiation back to space, thus enhancing the shortwave cloud forcing by 11.6 W m^{-2} to -62.7 W m^{-2}. At the same time, more longwave radiation is trapped in the Earth atmosphere system, increasing the longwave cloud forcing by 16.1 W m^{-2} to 41.1 W m^{-2}. Changes in liquid water clouds are much smaller and thus not shown.

The differences between ECHAM5-hom and ECHAM5-het are more modest. Here the ice crystal number concentration decreases by 16%, which reduces the shortwave and longwave cloud forcing by 0.6 and 1.1 W m^{-2}, respectively. The changes are smaller than in the previous version of the ECHAM4 GCM (Lohmann et al., 2004), because there are fewer aerosols in the upper troposphere in ECHAM4 (Lohmann et al., 2007). Thus, limiting heterogeneous freezing by the smaller amount of dust particles in ECHAM4 reduces the ice crystal number concentration more than in ECHAM5-het.

Annual zonal means of the vertically inte-

Tab. 2: Annual global mean cloud properties. Ice water path (IWP) has been derived from ISCCP data (Storelvmo et al., 2008). Water vapor mass (WVM) data stem from MODIS. N_i refers to the vertically integrated ice crystal number concentration. Total precipitation (P_{tot}) is taken from the Global Precipitation Climatology Project (Adler et al., 2003). Total cloud cover (TCC) is obtained from surface observations (Hahn et al., 1994), ISCCP (Rossow and Schiffer, 1999) and MODIS data (King et al., 2003). The shortwave (SCF), longwave (LCF) and net cloud forcing (CF) estimates are taken from Kiehl and Trenberth (1997). In addition estimates of LCF from TOVS retrievals (Susskind et al., 1997; Scott et al., 1999) and SCF retrievals from CERES (Kim and Ramanathan, 2008) are included.

Simulation	ECHAM5-hom	ECHAM5-het	ECHAM5-alpha	OBS
IWP, g m^{-2}	9.4	9.3	11.2	29
N_i, 10^{10} m^{-2}	0.38	0.32	4.2	
WVM, kg m^{-2}	26.1	25.7	28.8	25.1
TCC, %	68.6	66.4	72.5	62-67
P_{tot}, mm d^{-1}	2.95	2.99	2.56	2.74
SCF, W m^{-2}	-51.1	-50.5	-62.7	-46.5 to -50
LCF, W m^{-2}	25.0	23.9	41.1	22-30
CF, W m^{-2}	26.1	26.6	21.6	-19 to -27

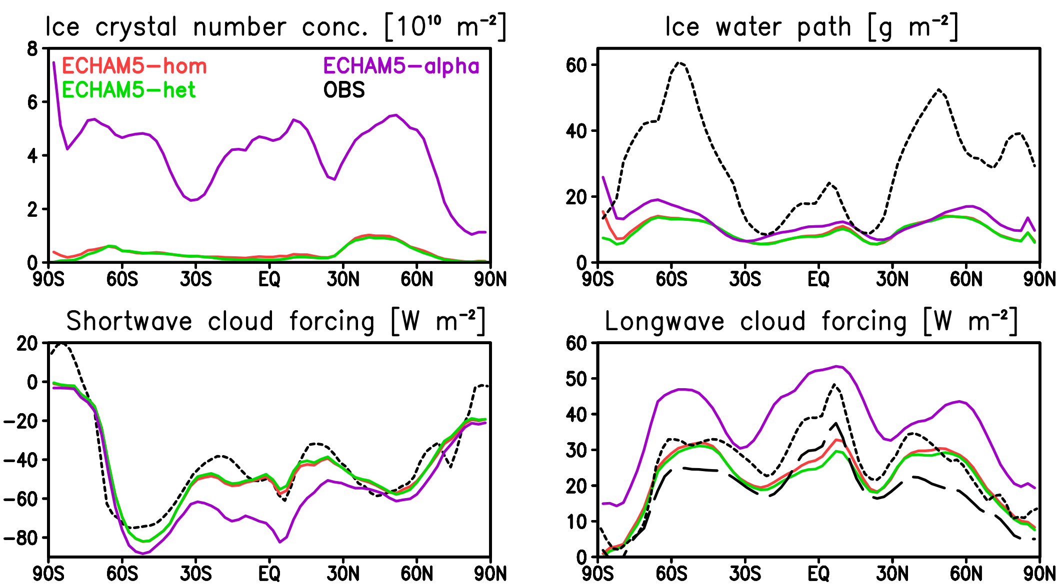

Fig. 1: Annual zonal means of ice water path, vertically integrated ice crystal number concentration, and of the shortwave and longwave cloud forcing from the different model simulations described in Table 1 and from observations described in Table 2. Dotted black lines refer to ISCCP data for IWP (Storelvmo et al., 2008) and to ERBE for the shortwave and longwave cloud forcing. The dashed line refers to TOVS data (Susskind et al., 1997; Scott et al., 1999).

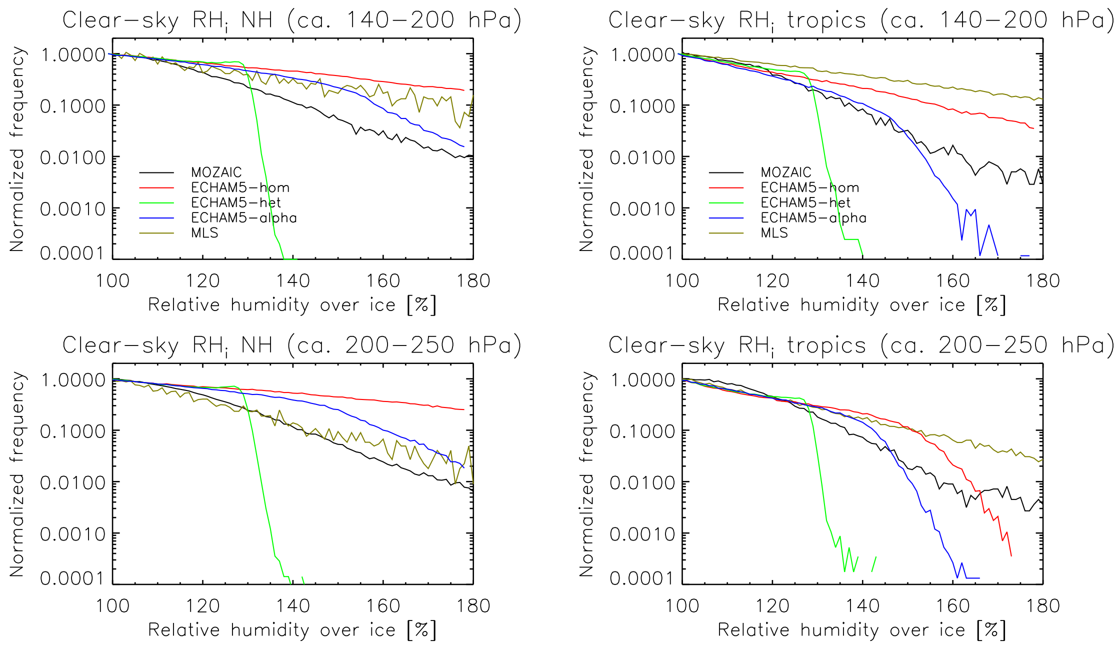

Fig. 2: Frequency of occurrence of relative humidity with respect to ice in the Northern Hemisphere (30°N-90°N) [left panel] and in the tropics (30°S-30°N) [right panel] in two different levels from MOZAIC aircraft data, MLS satellite data and from the simulations ECHAM5-hom, ECHAM5-het and ECHAM5-alpha.

grated ice crystal number concentration, ice water path, shortwave and longwave cloud forcing are shown in figure 1. Most noticeable is the smaller ice water path than observed and than simulated with the previous version of ECHAM5 (Lohmann et al., 2007). This is due to the changes to the model mentioned above. However, one has to bear in mind that the retrieval of the ice water path is very uncertain at this point. The shortwave and longwave cloud forcing of ECHAM5-hom and ECHAM5-het agree well with the observations, except that the longwave cloud forcing is underestimated in the topics. This suggests that the cirrus clouds are either not high enough or not thick enough. Given that the agreement was better in the previous version of ECHAM5 (Lohmann et al., 2007) where the ice water path was higher, the reduced ice water path is the likely cause for this discrepancy. Unfortunately there are no observations of the ice crystal number concentration, thus no conclusions about the right order of magnitude can be drawn.

The frequency of occurrence of different supersaturations with respect to ice in cloud-free regions has been obtained from MOZAIC aircraft data (Helten et al., 1998; Spichtinger et al., 2004) and MLS satellite data (Read et al., 2001; Spichtinger et al., 2003) (Figure 2). Both observational data suggest an exponential decrease for relative humidities with respect to ice (RH$_i$) for RH$_i$ above 100%. They differ in the slope, with the MLS slope being less steep.

In the simulations, we obtained RH$_i$ by restricting the analysis to grid boxes with less than 0.1 mg/kg condensate. In the Northern Hemisphere, the exponential decrease of RH$_i$ in simulation ECHAM5-hom is not as pronounced as suggested in the observations, especially as derived from MOZAIC data. The exponential decrease it better matched in the tropics, where it lies between the observational estimates. In simulation ECHAM5-alpha, the agreement with observations is better for RH$_i$ below 145% in the tropics and generally better than in simulation ECHAM5-hom in the Northern Hemisphere. This could suggest that the ice crystals in ECHAM5-hom sediment out too rapidly so that RH$_i$ cannot be sufficiently depleted. Simulation ECHAM5.5-het does not agree well with observations at RH$_i$ exceeding 130% because by design it depletes higher RH$_i$, while they are observed rather frequently in observations (Figure 2 and Peter et al. (2006)).

One difference between the MLS and MOZAIC observations is the cloud screening. While MLS is restricted to clear-skies (Spichtinger et al., 2003), MOZAIC detects supersaturation in cirrus clouds as well. Varying the threshold of cloud condensate in the model simulations does not affect the exponential slope significantly (not shown).

5 CONCLUSIONS

The homogeneous freezing scheme for cirrus clouds that was developed and tested in ECHAM4 has been incorporated into ECHAM5 (Lohmann et al., 2007). Here we tested its sensitivity with respect to the accommodation coefficient and with respect to heterogeneous versus homogeneous freezing.

The main findings are:

- If α is decreased from 0.5 to 0.005, then the ice crystal number concentration increases by one order of magnitude, while the impact on ice water content and cloud cover is much smaller.
- This changes the global annual mean shortwave and longwave cloud forcing by 12 and 16 W m^{-2}, respectively.
- The impact of heterogeneous freezing versus homogeneous freezing is much weaker with global annual mean changes of the shortwave and longwave cloud forcing by 0.6 and 1.1 W m^{-2}.

REFERENCES

Adler, R. F., Huffman, G. J., Chang, A., Ferraro, R., Xie, P. P., Janowiak, J., Rudolf, B., Schneider, U., Curtis, S., Bolvin, D., Gruber, A., Susskind, J., Arkin, P., Nelkin, E., 2003. The version-2 global precipitation climatology project (GPCP) monthly precipitation analysis (1979-present). J. Hydrometeor. 4 (6), 1147–1167.

Chen, T., Rossow, W. B., Zhang, Y. C., 2000. Radiative effects of cloud-type variations. J. Climate 13 (1), 264–286.

Cziczo, D. J., DeMott, P. J., Brooks, S. D., Prenni, A. J., Thomson, D. S., Baumgardner, D., Wilson, J. C., Kreidenweis, S. M., Murphy, D. M., 2004. Observations of organic species and atmospheric ice formation. Geophys. Res. Lett. 31, doi: 10.1029/2004GL019822.

Dymarska, M., Murray, B. J., Sun, L. M., Eastwood, M. L., Knopf, D. A., Bertram, A. K., 2006. Deposition ice nucleation on soot at temperatures relevant for the lower troposphere. J. Geophys. Res. 111 (D4).

Freud, E., Rosenfeld, D., Andreae, M. O., Costa, A. A., Artaxo, P., 2008. Robust relations between ccn and the vertical evolution of cloud drop size distribution in deep convective clouds. Atmos. Chem. Phys. 8 (6), 1661–1675.

Gettelman, A., Fetzer, E. J., Eldering, A., Irion, F. W., 2006. The global distribution of supersaturation in the upper troposphere from the atmospheric infrared sounder. J. Climate 19 (23), 6089–6103.

Hahn, C. J., Warren, S. G., London, J., 1994. Climatological data for clouds over the globe from surface observations, 1982-1991: The total cloud edition. Tech. rep., ORNL/CDIAC-72 NDP-026A Oak Ridge National Laboratory, Oak Ridge Tennessee, U.S.A.

Helten, M., Smit, H. G. J., Strater, W., Kley, D., Nedelec, P., Zoger, M., Busen, R., 1998. Calibration and performance of automatic compact instrumentation for the measurement of relative humidity from passenger aircraft. J. Geophys. Res. 103 (D19), 25643–25652.

Hoose, C., Lohmann, U., Erdin, R., Tegen, I., 2008. Global influence of dust mineralogical composition on heterogeneous ice nucleation in mixed-phase clouds. Environ. Res. Lett.In press.

Immler, F., Treffeisen, R., Engelbart, D., Krüger, K., Schrems, O., 2008. Cirrus, contrails, and ice supersaturated regions in high pressure systems at northern mid latitudes. Atmos. Chem. Phys. 8, 1689–1699.

Jensen, E. J., Pfister, L., Bui, T. V., Lawson, P., Baker, B., Mo, Q., Baumgardner, D., Weinstock, E. M., Smith, J. B., Moyer, E. J., Hanisco, T. F., Sayres, D. S., St. Clair, J. M., Alexander, M. J., Toon, O. B., Smith, J. A., 2008. Formation of large ($\sim 100\mu$m) ice crystals near the tropical tropopause. Atmos. Chem. Phys. 8, 1621–1633.

Kärcher, B., Hendricks, J., Lohmann, U., 2006. Physically based parameterization of cirrus cloud formation for use in global atmospheric models. J. Geophys. Res. 111 (D1), doi: 10.1029/2005JD006219, d01205.

Kärcher, B., Koop, T., 2005. The role of organic aerosols in homogeneous ice formation. Atmos. Chem. Phys. 5, 703–714.

Kärcher, B., Lohmann, U., 2002. A parameterization of cirrus cloud formation: Homogeneous freezing of supercooled aerosols. J. Geophys. Res. 107, doi: 10.1029/2001JD000470.

Kärcher, B., Lohmann, U., 2003. A parameterization of cirrus cloud formation: Heterogeneous freezing. J. Geophys. Res. 108, doi: 10.1029/2002JD003220.

Kiehl, J. T., Trenberth, K. E., 1997. Earth's annual global mean energy budget. Bull. Amer. Meteorol. Soc. 78 (2), 197–208.

Kim, D. Y., Ramanathan, V., 2008. Solar radiation budget and radiative forcing due to aerosols and clouds. J. Geophys. Res. 113, doi:10.1029/2007JD008434, d02203.

King, M. D., Menzel, W. P., Kaufman, Y. J., Tanre, D., Gao, B. C., Platnick, S., Ackerman, S. A., Remer, L. A., Pincus, R., Hubanks, P. A., 2003. Cloud and aerosol properties, precipitable water, and profiles of temperature and water vapor from MODIS. IEEE Trans. Geo. Rem. Sens. 41 (2), 442–458.

Liu, X., Penner, J. E., Ghan, S. J., Wang, M., 2007. Inclusion of ice microphysics in the ncar community atmospheric model version 3 (cam3). J. Climate 20, 4526–4547.

Liu, X. H., Penner, J. E., 2005. Ice nucleation parameterization for global models. Meteorol. Z. 14 (4), 499–514.

Lohmann, U., 2008. Global anthropogenic aerosol effects on convective clouds in ECHAM5-HAM. Atmos. Chem. Phys. 8, 2115–2131.

Lohmann, U., Kärcher, B., 2002. First interactive simulations of cirrus clouds formed by homogeneous freezing in the ECHAM GCM. J. Geophys. Res. 107, doi: 10.1029/2001JD000767, d4105.

Lohmann, U., Kärcher, B., Hendricks, J., 2004. Sensitivity studies of cirrus clouds formed by heterogeneous freezing in the echam gcm. J. Geophys. Res 109, 10.1029/2003JD004443, d16204.

Lohmann, U., Roeckner, E., 1996. Design and performance of a new cloud microphysics scheme developed for the ECHAM general circulation model. Clim. Dyn. 12, 557–572.

Lohmann, U., Stier, P., Hoose, C., Ferrachat, S., Kloster, S., Roeckner, E., Zhang, J., 2007. Cloud microphysics and aerosol indirect effects in the global climate model echam5-ham. Atmos. Chem. Phys. 7, 3425–3446.

Magee, N., Moyle, A. M., Lamb, D., 2006. Experimental determination of the deposition coefficient of small cirrus-like ice crystals near-50 degrees c. Geophys. Res. Lett. 33 (17).

Möhler, O. M., Buttner, S., Linke, C., Schnaiter, M., Saathoff, H., Stetzer, O., Wagner, R., Kramer, M., Mangold, A., Ebert, V., Schurath, U., 2005. Effect of sulfuric acid coating on heterogeneous ice nucleation by soot aerosol particles. Journal of Geophysical Research-Atmospheres 110 (D11), d11210.

Peter, T., Marcolli, C., Spichtinger, P., Corti, T., Baker, M. B., Koop, T., 2006. When dry air is too humid. Science 314 (5804), 1399–1401.

Pruppacher, H. R., Klett, J. D., 1997. Microphysics of Clouds and Precipitation. Kluwer Acad., Norwell, Mass.

Read, W. G., Waters, J. W., Wu, D. L., Stone, E. M., Shippony, Z., 2001. UARS Microwave Limb Sounder upper tropospheric humidity measurement: Method and validation. J. Geophys. Res. 106, 32,207–32,258.

Roeckner, E., Bäuml, G., Bonaventura, L., Brokopf, R., Esch, M., Giorgetta, M., Hagemann, S., Kirchner, I., Kornblueh, L., Manzini, E., Rhodin, A., Schlese, U., Schulzweida, U., Tompkins, A., 2003. The atmospheric general circulation model ECHAM5. part i: Model description. Tech. Rep. 349, Max-Planck-Inst. für Meteorol., Hamburg, Germany.

Rossow, W. B., Schiffer, R. A., 1999. Advances in understanding clouds from ISCCP. Bull. Amer. Meteorol. Soc. 80, 2261–2287.

Scott, N. A., Chedin, A., Armante, R., Francis, J., Stubenrauch, C., Chaboureau, J. P., Chevallier, F., Claud, C., Cheruy, F., 1999. Characteristics of the TOVS Pathfinder Path-B dataset. Bull. Amer. Meteorol. Soc. 80 (12), 2679–2701.

Spichtinger, P., Gierens, K., 2008. Modelling of cirrus clouds - Part 1: Model description and validation. Atmos. Chem. Phys. Discuss. 8, 601–686.

Spichtinger, P., Gierens, K., Read, W., 2003. The global distribution of ice-supersaturated regions as seen by the Microwave Limb Sounder. Q. J. R. Meteorol. Soc. 129, 3391–3410.

Spichtinger, P., Gierens, K., Smit, H. G. J., Ovarlez, J., Gayet, J. F., 2004. On the distribution of relative humidity in cirrus clouds. Atmos. Chem. Phys. 4, 639–647.

Stier, P., Feichter, J., Kinne, S., Kloster, S., Vignati, E., Wilson, J., Ganzeveld, L., Tegen, I., Werner, M., Balkanski, Y., Schulz, M., Boucher, O., Minikin, A., Petzold, A., 2005. The aerosol-climate model ECHAM5-HAM. Atmos. Chem. Phys. 5, 1125–1156.

Storelvmo, T., Kristjansson, J.-E., Lohmann, U., 2008. Aerosol influence on mixed-phase clouds in CAM-Oslo. J. Atmos. Sci.In press.

Sundqvist, H., Berge, E., Kristiansson, J. E., 1989. Condensation and cloud parameterization studies with a mesoscale numerical weather prediction model. Mon. Wea. Rev. 117, 1641–1657.

Susskind, J., Piraino, P., Rokke, L., Iredell, T., Mehta, A., 1997. Characteristics of the TOVS Pathfinder Path A dataset. Bull. Amer. Meteorol. Soc. 78 (7), 1449–1472.

Wood, S. E., Baker, M. B., Calhoun, D., 2001. New model for the vapor growth of hexagonal ice crystals in the atmosphere. J. Geophys. Res. 106, 4845–4870.